

Received August 25, 2017, accepted September 29, 2017, date of publication October 12, 2017, date of current version November 7, 2017.

Digital Object Identifier 10.1109/ACCESS.2017.2760924

Steerable Higher Order Mode Dielectric Resonator Antenna With Parasitic Elements for 5G Applications

NOR HIDAYU SHAHADAN^{1,2}, MOHD HAIZAL JAMALUDDIN^{1b2}, (Member, IEEE), MUHAMMAD RAMLEE KAMARUDIN^{1b3}, (Senior Member, IEEE), YOSHIHIDE YAMADA⁴, (Senior Member, IEEE), MOHSEN KHALILY^{1b5}, (Member, IEEE), MUZAMMIL JUSOH⁶, (Member, IEEE), and SAMSUL HAIMI DAHLAN⁷

¹Department of Electrical Engineering, Politeknik Ibrahim Sultan, Pasir Gudang 81700, Malaysia

²Wireless Communication Centre, Faculty of Electrical Engineering, Universiti Teknologi Malaysia, Skudai 81310, Malaysia

³Centre for Electronic Warfare Information and Cyber, Cranfield Defence and Security, Cranfield University, Defence Academy of the United Kingdom, Shrivenham SN6 8LA, U.K.

⁴Malaysia-Japan International Institute of Technology, Universiti Teknologi Malaysia, Kuala Lumpur 54100, Malaysia

⁵Home of the 5G Innovation Centre, Department of Electronic Engineering, Institute for Communication Systems, University of Surrey, Guildford GU2 7XH, U.K.

⁶School of Computer and Communication Engineering, Universiti Malaysia Perlis, Pauh Putra 02600, Malaysia

⁷Electromagnetic Compatibility Center, Universiti Teknologi Tun Hussein Onn, Parit Raja 86400, Malaysia

Corresponding author: Muhammad Ramlee Kamarudin (ramlee.kamarudin@cranfield.ac.uk)

This work was supported in part by the Ministry of Education Malaysia and in part by Universiti Teknologi Malaysia under Grant HiCOE (4J220 and 4J211), Grant FRGS (4F733 and 4F283), and Grant UTM GUP (05H62, 03G33, 13H26, and 11H59).

ABSTRACT This paper presents the findings of a steerable higher order mode (TE_{183}^y) dielectric resonator antenna with parasitic elements. The beam steering was successfully achieved by switching the termination capacitor on the parasitic element. In this light, all of the dielectric resonator antennas (DRAs) have the same dielectric permittivity similar to that of ten and excited by a 50Ω microstrip with a narrow aperture. The effect of the mutual coupling on the radiation pattern and the reflection coefficient, as well as the array factor, was investigated clearly using MATLAB version 2014b and ANSYS HFSS version 16. As the result, the antenna beam of the proposed DRA array managed to steer from -32° to $+32^\circ$ at 15 GHz. Furthermore, the measured antenna array showed the maximum gain of 9.25 dBi and the reflection coefficients which are less than -10 dB with the bandwidth more than 1.3 GHz, which is viewed as desirable for device-to-device communication in 5G Internet of Things applications.

INDEX TERMS Beam steering, dielectric resonator antenna, higher order mode, parasitic element, phased array, 5G.

I. INTRODUCTION

Telecommunication innovation has advanced quickly from the original (1G) to the fifth generation (5G) due to the expanding interest in boundless access to data and sharing of information. These features are very salient for many applications related to Internet of Things (IoT) such as Device-to-Device (D2D) communications as depicted in Fig. 1 [1]. Consequently, the increase of usage and the demand for simultaneous communication between devices cause interference, especially at higher frequencies in 5G. Therefore, a smart device embedded with wide bandwidth and high gain antenna is required to encounter the increasing traffic

demands and to address the interference problems [2], [3]. In addition, a directional antenna is also indispensable to satisfy the necessities of a long distance communication [4]. Recently, the spectrum above 6 GHz has gained so much attention for future networks and also viewed as a potential frequency for 5G applications [5]. Hence, the operating frequency of the antenna is proposed at 15 GHz.

In the meantime, the Friis formula advocates that the path loss is dependent on the frequency. Therefore, the loss will be increased at higher frequencies because of the decreased wavelength, and multiple antennas in the phased array that is capable of steering the direction beam with high gain can

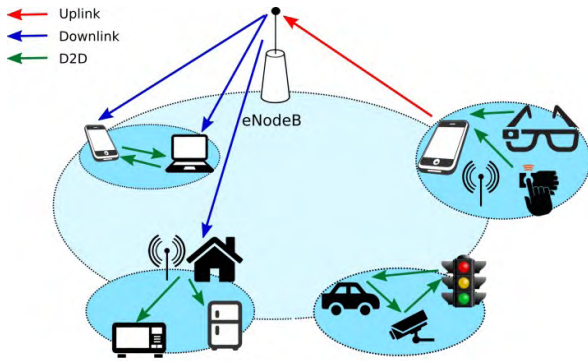


FIGURE 1. D2D communications in 5G Internet of Things (IoT) [1].

be used to recover the additional loss as well as to support access and the reconfigurable backhaul link [6]. Nevertheless, the complex phased array design that incorporates power distribution network, phase shifter and bias component has produced a larger overall dimension, where the sizes of the phased array design in [7] and [8] were more than $70 \text{ mm} \times 70 \text{ mm}$ at 10 GHz and 8 GHz, respectively, with the best reflection coefficient only at -18 dB [7]. Meanwhile, phase shifters are expensive and need intricate feeding networks that will introduce more losses at higher frequencies [9], hence, new phased arrays need to be developed by using different techniques. Past studies had reported the developments of beam steering antenna without the phase shifters requirement [10]–[13]. It is known as the electronically steerable passive array radiator (ESPAR) antenna that was excited by one of the elements in the array, called driven element, while others (parasitic elements) were excited by the mutual coupling of the driven element and were terminated with the capacitor loading. Furthermore, the phase shifts requisite for the steerable beam can be tuned by controlling the capacitor value on the parasitic elements.

Past researchers had conducted ESPAR investigations on patch elements [11] and wire [10]. However, the microstrip ESPAR had a limited steer angle at the boresight direction, while the steerable beam in [9] just reached the angle of $\pm 20^\circ$ and in [12], it reached $\pm 15^\circ$. Besides that, the microstrip ESPAR has a narrow impedance bandwidth and the performance of antenna gain was not more than 8.0 dBi [13]–[15]. Thus, in comparison to the microstrip antennas, the dielectric resonator antennas have shown various benefits, such as wider bandwidth and low loss that make it suitable for higher frequencies applications [16]. In recent years, the dielectric resonator antenna (DRA) ESPAR was fed through the microstrip line [17], which is typically excited in the fundamental mode. It does not take into consideration the effect of mutual impedance by the difference distance between DR and the H -field distribution inside the DR. Despite that, the impedance bandwidth between DRA ESPAR in [17] and microstrip ESPAR in [12] were more or less the same. Influenced by the higher-order mode DRA that manage to increase the gain and bandwidth of the single element [18], thus, it has proposed as a driven element in DRA array.

A preliminary study [19] has conducted a basic analysis through simulation. Despite the design's improved bandwidth and gain compared to other previous works, there are still drawbacks in the capability of the steering angle at $\pm 26^\circ$ and a broader half-power beamwidth (HPBW) at 112° . Thus, this study proposes an improvement of the concept presented [19], which will significantly modify the excitation mode of the parasitic elements. To the best of author's knowledge there are still no studies that used the higher-order mode (TE_{183}^y) together with the fundamental mode (TE_{181}^y) in the ESPAR design, hence, detailed analyses which included numerical and simulations were performed on both the proposed design and the previous work in [19]. As a result, better performance was substantially obtained when the configuration composed of the driven element excited in the TE_{183}^y mode while the parasitic elements were excited in the TE_{181}^y mode. In this paper, the proposed DRA array had achieved the beam steering angle from -32° to $+32^\circ$ with the measured bandwidth of more than 1.3 GHz, specifically at 15 GHz without a need of phase shifters. Furthermore, the antenna gain had increased as the steering angle increased and achieved the maximum measured gain at 9.25 dBi with 61° of HPBW. In this regard, the proposed DRA array presents a potential candidate for 5G (IoT) applications which could be applied to Device-to-Device (D2D) communication.

This paper is organized as follow, first, the comparisons between the single DRA excited in the higher-order mode (TE_{183}^y) and the fundamental mode (TE_{181}^y) are analyzed in Section II, followed by the comparison analysis between the designed in [19] and the proposed design. Furthermore, the chapter will explain the investigation in regards to the beam steering in theory and based on the simulation, as well as the six controlling ideal switches embedded in the feed line of the parasitic elements to manage the beam switching. In the meantime, Section III presents the fabricated design and compares its measurement results with the simulation. Finally, Section IV will conclude the discussion in the paper.

II. DESIGN AND ANALYSIS

A. ANTENNA CONFIGURATION

The geometry of the single element rectangular DRA with the dimension w , d and h is shown in Fig. 2. The resonant frequencies, f_0 of the $\text{TE}_{m\delta n}^y$ with a dielectric constant, ϵ_r can be predicted using (1) derived from the dielectric waveguide model [20]. The following equations are acquired for the wavenumber k_x , k_y , and k_z where m and n are index numbers.

$$\begin{aligned} k_x &= m\pi/d, \\ k_y \tan\left(\frac{k_y w}{2}\right) &= \sqrt{(\epsilon_r - 1)k_0^2 - k_y^2}, \\ k_z &= n\pi/2h \end{aligned} \quad (1)$$

where k_0 denotes the wavenumber of the free space at 15 GHz.

The higher-order mode was introduced by increasing the dimension of the antenna in a direction normal to ground

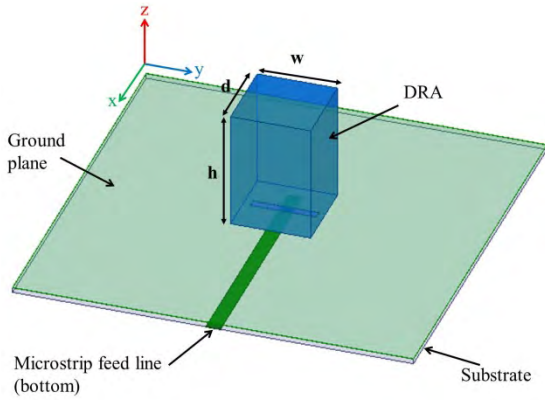


FIGURE 2. Geometry of the single element DRA.

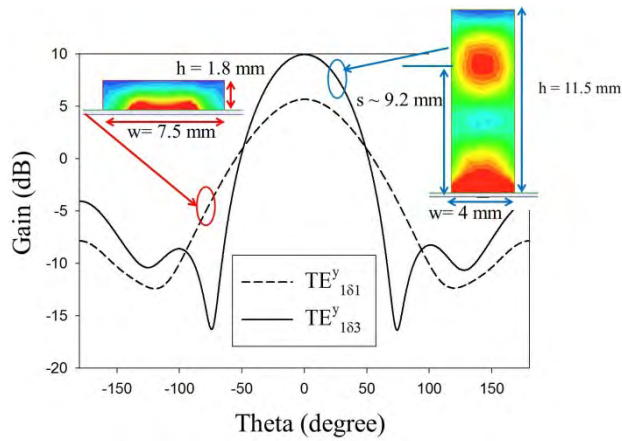


FIGURE 3. Simulated H_y -field and radiation pattern of the single DRA at 15 GHz.

plane, which offers a higher gain till the non-occurrence of the overlap dipole. Hence, the theory of short magnetic dipoles was used to define the modes in the minimum spacing, s between the short magnetic dipoles should be equal to 0.4λ [21]. Fig. 3 shows the simulated H_y field of the single DRA at 15 GHz by exciting in the fundamental mode (TE_{181}^y) and the higher-order mode (TE_{183}^y). The TE_{183}^y mode was approximately spaced, with $s = 9.2$ mm apart which correspond to 0.46λ . Therefore, the gain for the single DRA excited in TE_{183}^y mode had achieved 9.95 dBi of the antenna gain, which is 2 times higher than the TE_{181}^y mode. In addition, the directivity of the single DRA in TE_{183}^y mode achieved 9.97 dB which is better than TE_{181}^y mode. Hence, in order to increase the antenna bandwidth, the TE_{183}^y mode DR was placed on the ground plane side and fed by a 50 Ω microstrip line through a narrow aperture in the ground plane with the strongest amount of the aperture coupling, χ [20]. In this light, by optimize the width of the slot (W_s), the length of the stub (S), and the width of the microstrip line (W), it was reduced the loaded Q -factor in (2), thus increased the antenna bandwidth even though in the higher-order mode [18]. In contrary with the work in [21], the TE_{183}^y mode DRA in the proposed design has attained a wider impedance bandwidth

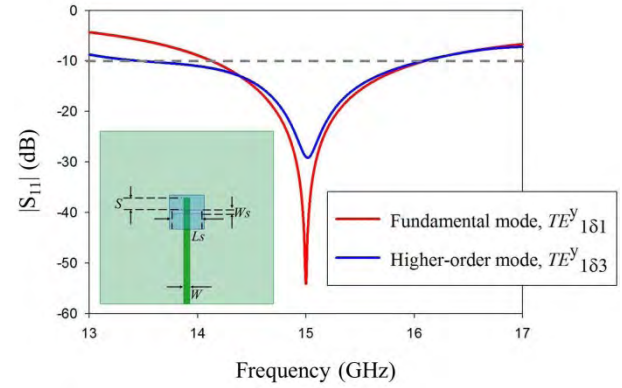


FIGURE 4. Comparison of the impedance bandwidth.

compared to the TE_{181}^y mode as shown in Fig. 4.

$$Q_L = \frac{Q}{1 + \chi} \quad (2)$$

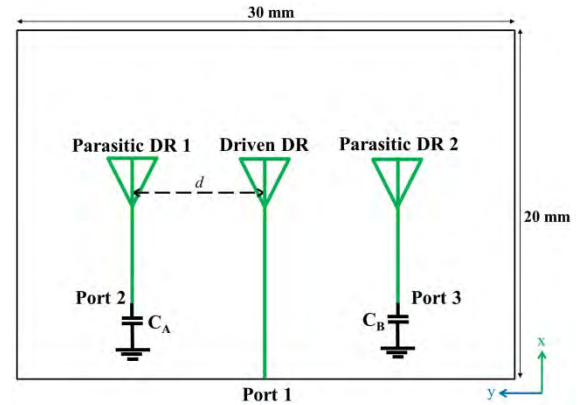


FIGURE 5. Layout of DRA arrays with driven and parasitic.

Next, an array which consist of three elements dielectric resonators (DRs) was designed as shown in Fig. 5. The beam can be steered by adjusting the value C_A and C_B at port 2 and port 3, respectively. The analysis was compared between the designed in [19] and the proposed design as tabulated in Table 1. The TE_{183}^y mode was designated as a driven DR due to its intriguing advantages in gain and bandwidth, compared to TE_{181}^y mode [18]. Nevertheless, the effects to the antenna performance through the use of different excitation mode of the parasitic DRs will be investigated and analyzed in the next section.

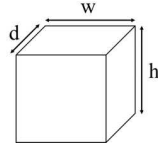
B. EFFECTIVE DISTANCE, d BETWEEN THE DIELECTRIC RESONATORS

The driven DR and each of the parasitic DRs were separated by the distance, d . This distance influenced a mutual coupling effect to excite the parasitic DRs (port 2 and port 3) from the driven DR (port 1). Interestingly, this array needs a stronger mutual coupling so that a larger of current ratio between

TABLE 1. Configuration of three element DRs.

Design	Proposed	[19]
Driven DR	Higher-order mode, TE_{183}^y	Higher-order mode, TE_{183}^y
Parasitic DR1	Fundamental mode, TE_{181}^y	Higher-order mode, TE_{183}^y
Parasitic DR2	Fundamental mode, TE_{181}^y	Higher-order mode, TE_{183}^y

DR dimensions



Note: TE_{181}^y , ($w = d = 7.5$ mm, $h = 1.8$ mm) and TE_{183}^y , ($w = d = 4$ mm, $h = 11.5$ mm)

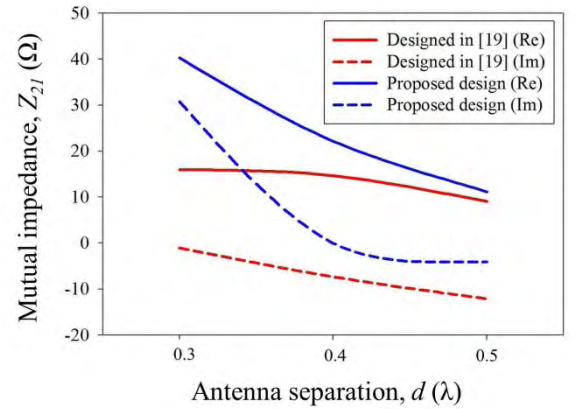
the DR can be obtained, which also influenced the capabilities of the steerable beam. In this regard, a preliminary study on the mutual impedance, Z_{21} and the reflection coefficients were performed to determine the effective distance, d . In order to analyze the coupling effect between the elements, all ports were activated to extract the Z parameters from ANSYS High Frequency Structural Simulator version 16.0 (HFSS). Meanwhile, in reference to Fig. 6(a), the mutual impedance, Z_{21} which also represent Z_{31} between the parasitic DR and the driven DR for both design had increased when the distance, d was decreased from 0.5λ to 0.3λ . However, the proposed design showed the higher mutual impedance compared to the designed in [19] due the closer separation between edges of the driven DR to the edge of the parasitic DR. Meanwhile, while the closer d resulted in stronger mutual coupling and will increase in the current magnitude and phase shifting, Fig. 6(b) illustrates that there was a mismatch impedance which occurred at particular 15 GHz for $d = 0.3\lambda$. Accordingly, $d = 0.4\lambda$ (8mm) was selected as the effective distance between the DRs.

C. THEORETICAL BASIS OF BEAM STEERING

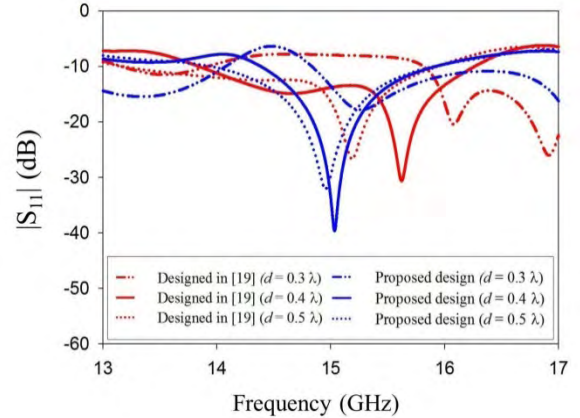
The DRA array can be synthesized with three-port network theory in [17] and the current ratio between the parasitic DR and the driven DR was obtained through (3):

$$\begin{pmatrix} \frac{I_2}{I_1} \\ \frac{I_3}{I_1} \end{pmatrix} = \begin{pmatrix} Z_{22} + Z_{CA} & Z_{23} \\ Z_{23} & Z_{33} + Z_{CB} \end{pmatrix}^{-1} \begin{pmatrix} -Z_{21} \\ -Z_{31} \end{pmatrix} \quad (3)$$

Since the capacitance, C_A and C_B are the main directories for the steerable beam, the distributions of $|I_2/I_1|$ and $|I_3/I_1|$ on the parasitic DRs can be controlled by adjusting their values. The range of 0.01 pF – 1 pF was predicted in [19] as the operational capacitances that would impact the steering beam of the proposed antenna.



(a)



(b)

FIGURE 6. (a) Characteristics of the mutual impedance (Z_{21}) with various distance, d . (b) Characteristics of the reflection coefficients with various distance, d

The numerical investigation was done for both designs by varying the capacitance C_B with constant value $C_A = 0.01$ pF to observe the effect of the current ratio and the phase difference between the parasitic elements. Subsequently, Fig. 7(a) and Fig. 7(b) show that the current ratio $|I_3/I_1|$ and the phase difference for both designs could be increased by increasing the capacitance value C_B . Nevertheless, the proposed design produced a higher $|I_3/I_1|$ and phase difference compared to the designed in [19]. Hence, the array factor of the phased array can be calculated by using (4):

$$AF = 1 + \left| \frac{I_2}{I_1} \right| e^{-j(0.8\pi \sin \theta - \beta_1)} + \left| \frac{I_3}{I_1} \right| e^{-j(0.8\pi \sin \theta - \beta_2)} \quad (4)$$

Subsequently, once the AF is known, the radiation pattern of the phased array can be obtained. The normalized AF from the numerical calculation is shown in the Fig. 8 and it indicates that the beam steering of the proposed design is theoretically possible. It can also be observed that, the AF is almost constant for both design when $C_A = C_B = 0.01$ pF because of the little current in the parasitic DRs. As expected, the numerical analysis shows that the proposed design had achieved a better steering capability influenced by a stronger mutual coupling in that configuration.

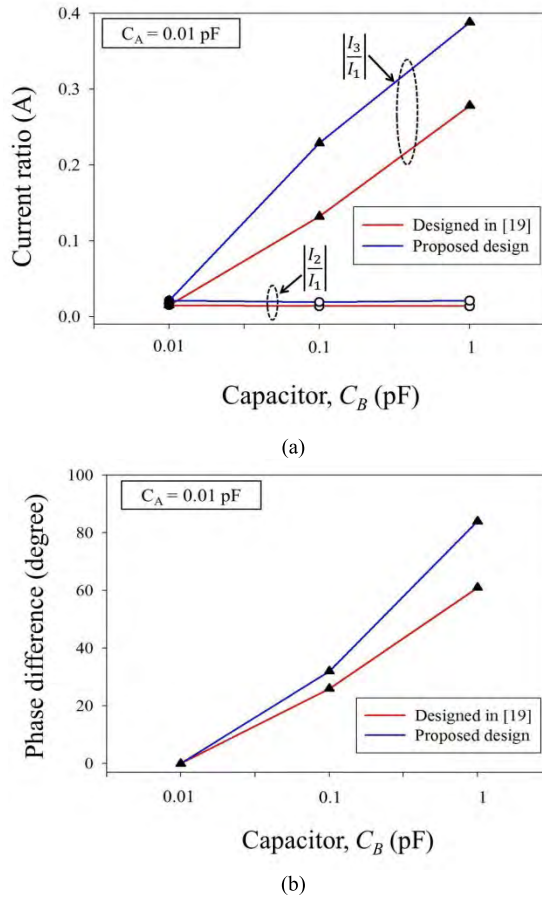


FIGURE 7. (a) Variation of the current ratio with capacitance, C_B . (b) Variation of the phase difference with capacitance, C_B .

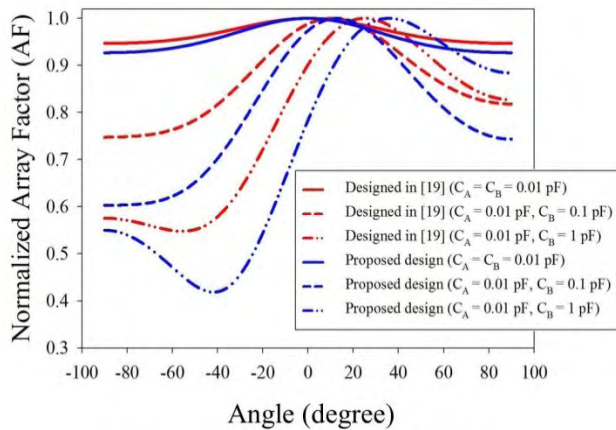


FIGURE 8. Normalized array factor (AF) with the capacitive load.

D. SIMULATED ANALYSIS OF BEAM STEERING

Figure 9 presents comparison of the simulated result between the designed in [19] and the proposed design for three different steering angles. Consequently, when C_A and C_B used the smallest capacitor value (0.01 pF), the reactance $Z_{CA} = 1/j\omega C_A$ and $Z_{CB} = 1/j\omega C_B$ at the both parasitic elements would be increased. Therefore, this led to the ratio of $|I_2/I_1|$ and $|I_3/I_1|$ to zero and indirectly inclines the input impedance

TABLE 2. Switching configuration for various cases.

		Case I	Case II	Case III	Case IV	Case V
Parasitic DR1	SW1	ON	OFF	ON	OFF	ON
	$C_1 = 0.01$ pF					
	SW2	OFF	OFF	OFF	ON	OFF
	$C_3 = 1$ pF					
Parasitic DR2	SW3	OFF	ON	OFF	OFF	OFF
	$C_2 = 0.1$ pF					
	SW4	OFF	OFF	ON	OFF	OFF
	$C_2 = 0.1$ pF					
	SW5	OFF	OFF	OFF	OFF	ON
	$C_3 = 1$ pF					
	SW6	ON	ON	OFF	ON	OFF
	$C_1 = 0.01$ pF					

to the impedance value itself. This caused the beam direction to be at 0° as shown in Fig. 9(b). Meanwhile, when C_B value was bigger than C_A , the loading reactance, Z_{CB} would be near to the short circuit state. Thus, the ratio $|I_3/I_1|$ changed rapidly and afterward, diverged the input impedance Z_{in} from the impedance value itself. Consequently, the beam was directed to the positive degrees as depicted in Fig. 9(c). The opposite reaction will happen if the value of C_A is bigger than C_B , as shown in Fig. 9(a).

In reference to Fig. 9, it is clearly indicated that the proposed design not only had achieved a better steering capability as expected in the theoretical analysis, but has shown a narrower HPBW compared to [19]. Apparently, this occurred due to the H -field distribution influence inside the DR, as depicted in Fig. 10 (designed in [19]) and in Fig. 11 (proposed design). Fig. 10 shows the H -field inside the parasitic DRs excited in the TE_{183}^y mode have deteriorated the steerable beam, thus increased the HPBW of the antenna. This did not happen in the proposed design which applied the parasitic DRs excited in the TE_{181}^y mode. Consequently, the antenna gain from the proposed design had increased with the increase the steering angle, contrary to the designed in [19], as shown in Fig. 12.

E. GEOMETRICAL DETAILS FOR BEAM STEERING OF THE PROPOSED ANTENNA

Based on the detailed comparison of the theoretical and simulation analyses conducted, this paper can deduce that the proposed design has a better performance compared to the designed in [19], hence, the proposed DRA arrays design with $\epsilon_r = 10$ and the layout are shown in Fig. 13. The structure consists of a slot aperture that etched on the Duroid 5880 dielectric substrate with a permittivity, ϵ_s of 2.2, thickness, t_s of 0.254 mm, and a loss tangent, δ of 0.001. In addition, the shorting pins were applied to connect the ground plane. In this light, the switching configuration to terminate the parasitic elements with the suitable capacitor is tabulated in Table 2, where the OFF and ON conditions specified the open-circuit and short-circuit between the parasitic element and the relative capacitor, respectively.

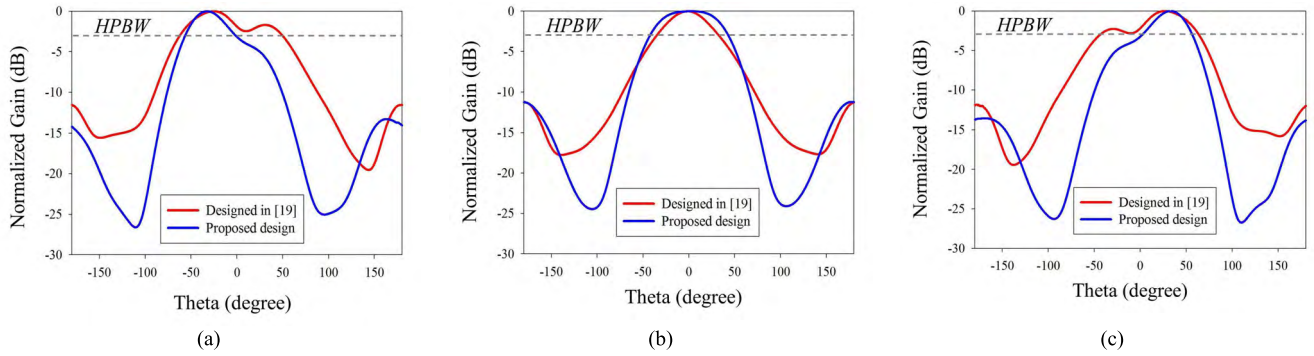


FIGURE 9. Comparison of the simulated radiation pattern at H -plane (a) $C_A = 1$ pF, $C_B = 0.01$ pF. (b) $C_A = C_B = 0.01$ pF (c) $C_A = 0.01$ pF, $C_B = 1$ pF.

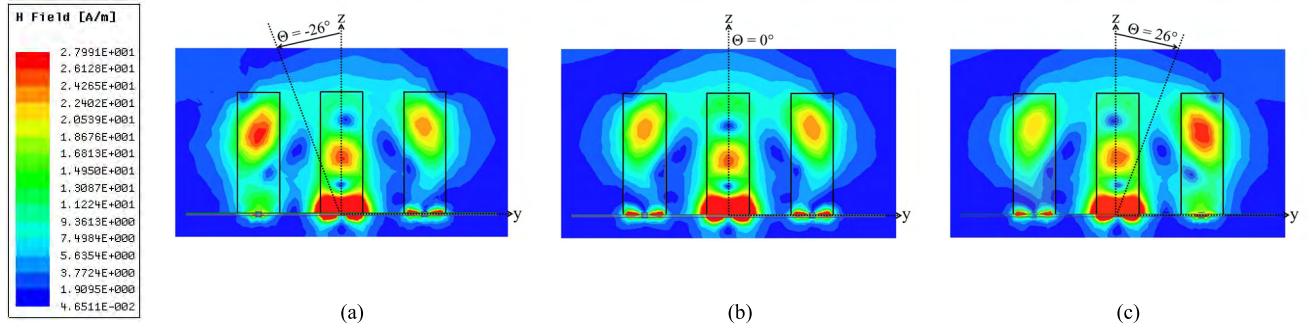


FIGURE 10. H_y -field distribution of the designed in [19] (a) $C_A = 1$ pF, $C_B = 0.01$ pF. (b) $C_A = C_B = 0.01$ pF. (c) $C_A = 0.01$ pF, $C_B = 1$ pF.

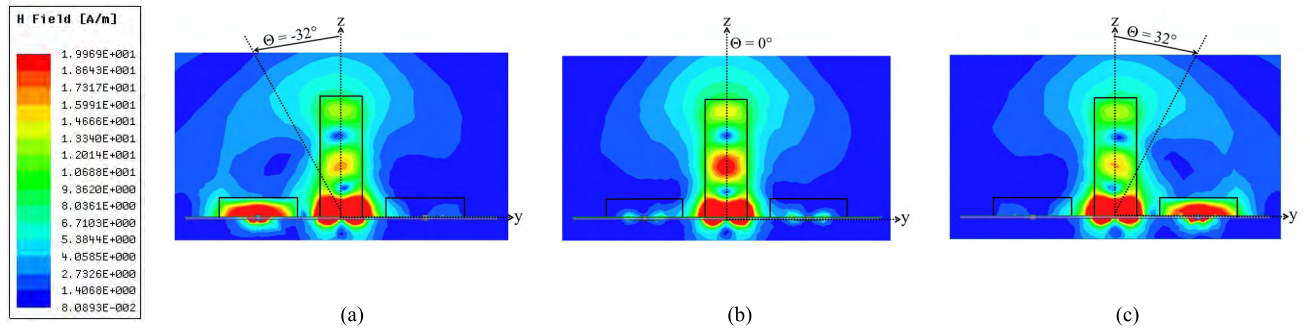


FIGURE 11. H_y -field distribution of the proposed designed (a) $C_A = 1$ pF, $C_B = 0.01$ pF. (b) $C_A = C_B = 0.01$ pF. (c) $C_A = 0.01$ pF, $C_B = 1$ pF.

III. RESULTS AND DISCUSSIONS

The proposed DRA array with switching configuration was fabricated and the photograph of the prototype is shown in Fig. 14. The DRs of the prototype were fabricated with the ECCOSTOCK HiK dielectric material ($\epsilon_r = 10$) while the feeding network was fabricated by etching the substrate of Duroid 5880 ($\epsilon_s = 2.2$). Meanwhile, the special type of double-sided duct tape with thickness about 0.05 mm is used to attach the DR to the ground plane. The DRs were painstakingly aligned on the ground plane slot by using the tracing paper as depicted in Fig. 14(a). This enhances the accuracy of the DR position since the misalignment between the DR and the feeding network is minimized. For comparison, the simulated and measured reflection coefficient

reactions with different cases are depicted in Fig. 15. It can be perceived that there is a slight difference in the simulated and measured bandwidth due to the fabrication tolerance of the DR and the signal deterioration by applying real capacitor as the switching component. However, the measured reflection coefficients for all cases were less than -10 dB across bandwidth exceeding 1.3 GHz. This exhibits a stable impedance matching and fulfills the bandwidth for 5G requirements. It is also worth mentioning that the proposed design has an overall size 30 mm \times 20 mm which is more compact than [7], [8] and better reflection coefficients compared to [7], which used phase shifters.

The capability of the steerable beam at the H -plane was also observed in five various cases and it has been illustrated

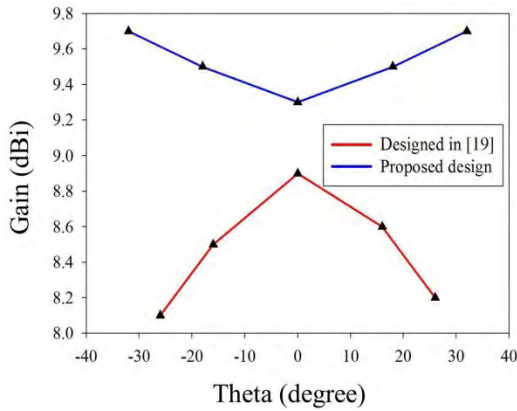


FIGURE 12. Comparison of the simulated gain.

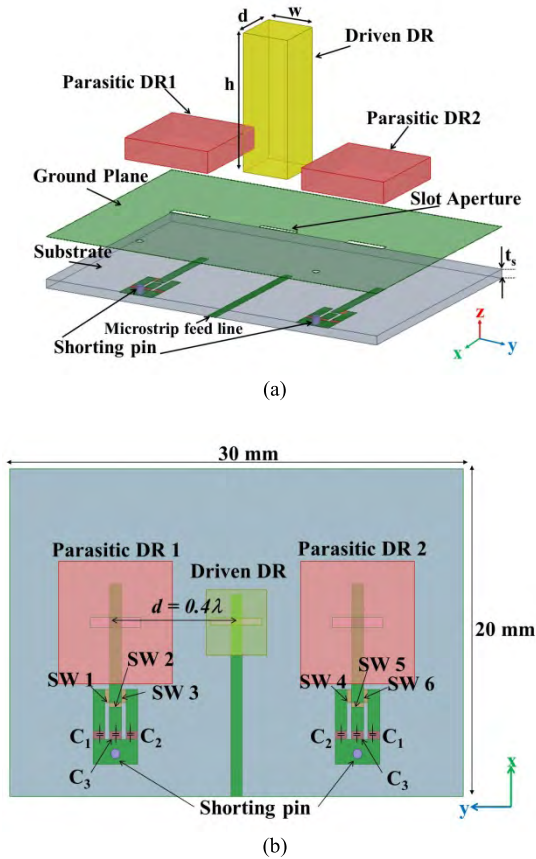


FIGURE 13. The geometrical configuration of the proposed DRA array (a) 3D view. (b) Top view.

with a stable radiation pattern across a bandwidth as presented in Fig. 16. A change in main beam radiation angle from -32 to $+32$ degrees was achievable by switching the termination capacitor on the parasitic element, as shown in Fig. 13(b). Since the radiation pattern of the array is obtained by multiplying the radiation pattern of a single element with the array factor, it has affected the HPBW for each angle due to the difference value of capacitor termination. In this light, when the beam is steered, the HPBW is reduced from 75° to 61° . It should also be noted that a PIN diode with a suitable DC bias network can be used for a continuous steering capability.

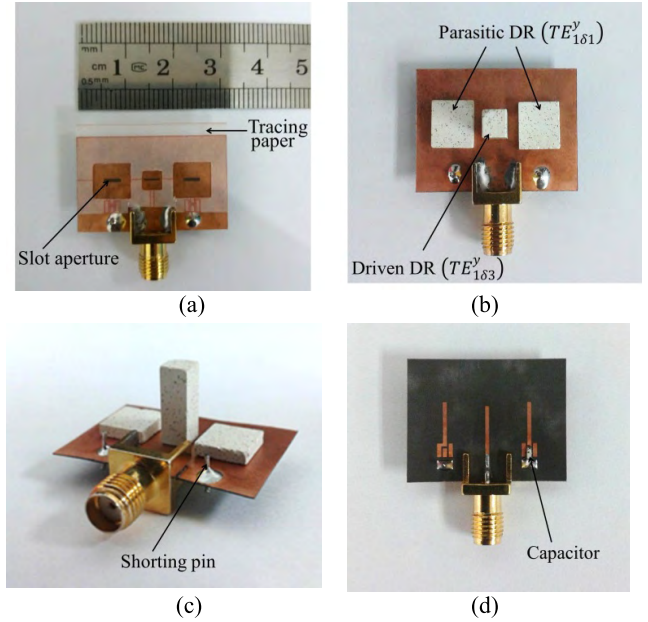


FIGURE 14. A prototype of the fabricated antenna. (a) Top view without DR. (b) Top view with DR. (c) 3D view. (d) Back view.

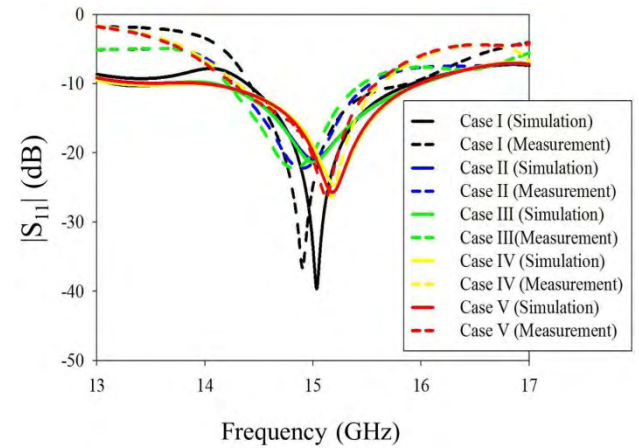


FIGURE 15. The simulated and measured reflection coefficients for various cases.

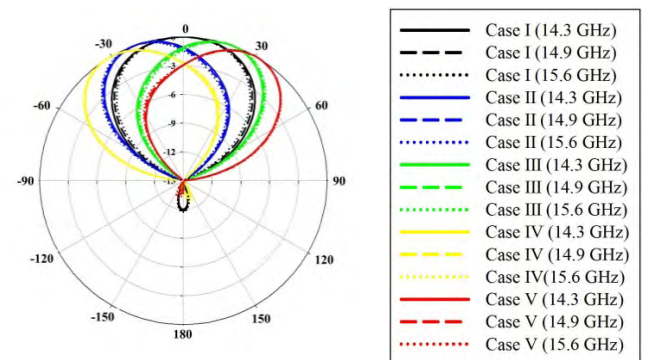


FIGURE 16. Simulated normalized beam pattern across a bandwidth.

Subsequently, it was observed in Fig. 17 that simulated and measured beam was steered approximately at the same angle, while the observed differences between the simulated

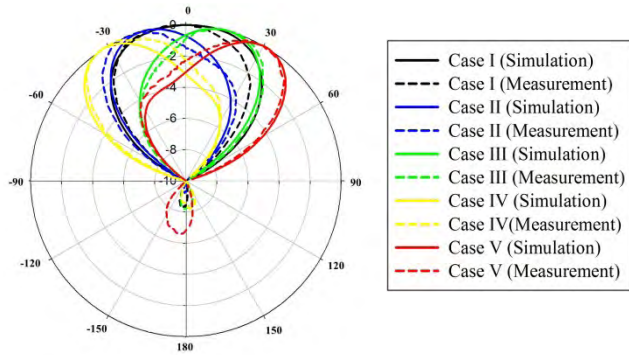


FIGURE 17. Simulated and measured normalized beam pattern for various cases at 15 GHz.

TABLE 3. Simulated and measured results for various cases.

		Case I	Case II	Case III	Case IV	Case V
Gain (dBi)	Simulation	9.17	9.57	9.55	9.84	9.77
	Measurement	8.45	8.95	8.85	9.25	9.15
Steering angle ($^{\circ}$)	Simulation	0	-18	+18	-32	+32
	Measurement	0	-19	+19	-32	+32
HPBW (deg)	Simulation	76	64	65	56	58
	Measurement	75	67	68	61	62

TABLE 4. Performance of the proposed DRA array compared to the previous work.

Design	Frequency (GHz)	Element no.	Driven element dimension (w x d x h) (mm)	Maximum Gain (dBi)
[9]	3	3	0.35λ x 0.28λ	Not mentioned
[11]	0.9	5	0.28λ x 0.25λ	6
[12]	1	3	0.26λ x 0.3λ	7.5
[17]	2.8	3	0.16λ x 0.16λ x 0.1λ	8.9
[19]	15	3	0.2λ x 0.2λ x 0.58λ	8.9
Proposed	15	3	0.2λ x 0.2λ x 0.58λ	9.25

Design	Bandwidth (GHz)	Steering angle (deg)	HPBW (deg)
[9]	0.05	±20	Not well-defined
[11]	0.01	±28	50° → 98°
[12]	0.07	±15	~80°
[17]	0.13	±30	90° → 75°
[19]	2.0	±26	68° → 112°
Proposed	1.3	±32	75° → 61°

and measured gain were in the range of 0.45 – 0.72 dBi only. Meanwhile, this DRA array was able to switch at five various steering angles: 0° , -19° , $+19^{\circ}$, -32° and $+32^{\circ}$ as tabulated in Table 3. It is also noted that the antenna gain had increased when the steering angle increased and in turn, the directivity of the antenna array was also increased. Besides that, by considering the simulated directivity and measured gain, this DRA array produced the acceptable values of the radiation efficiency of 92%, 93%, 92%, 93% and 93% for Case I, Case II, Case III, Case IV and Case V, respectively.

Hereby, it is worth specifying that integrated the higher-order mode, TE_{183}^y DR as a driven element together with the fundamental mode, TE_{181}^y DR as the parasitic element was increased the mutual impedance between the elements even though the antenna separation, d is approximately the same with [19]. Additionally, when the beam is steered, the

H -field distribution inside the parasitic DR cannot deteriorate the H -field inside the driven DR due to the different excitation mode. This leads the proposed design achieved a higher antenna gain, wider steering angle, and narrow HPBW in comparison with [19]. As an outcome, the proposed DRA array is superior to some of the previous works as tabulated in Table 4. Although the driven element dimension in the proposed design has a little higher compared to previous work, however, it is capable to steer the beam with a higher gain by exciting in the TE_{183}^y mode instead of adding more antenna element.

IV. CONCLUSION

This paper has presented the beam steering capabilities based on an array of three elements DRA with capacitor loading. Furthermore, TE_{183}^y mode DR was applied as a driven element with a narrow aperture in the ground plane achieved for a wider bandwidth more than 1.3 GHz and antenna gain in the range of 8.45 dBi to 9.25 dBi. This design attained $\pm 32^{\circ}$ steering abilities by switching the termination capacitor at parasitic DR exciting in TE_{181}^y mode without the need of a phase shifter. It can be considered that this proposed DRA array can be potentially applied for Device-to-Device (D2D) communication in 5G Internet of Things (IoT) applications. In the future work, this DRA array can be incorporated as a sub-array in a linear or planar array [22], [23], which will increase the directivity and gain, with a narrower HPBW.

REFERENCES

- [1] L. Militano, G. Araniti, M. Condoluci, and A. Iera, "Device-to-device communications for 5G Internet of Things," *EAI Endorsed Trans. Internet Things*, vol. 1, no. 1, pp. 1–15, 2015.
- [2] O. Bello and S. Zeadally, "Intelligent device-to-device communication in the Internet of Things," *IEEE Syst. J.*, vol. 10, no. 9, pp. 1172–1182, Sep. 2016.
- [3] S. Okasaka et al., "Proof-of-concept of a millimeter-wave integrated heterogeneous network for 5G cellular," *Sensors*, vol. 16, no. 9, pp. 1–21, 2016.
- [4] F. Boccardi, R. W. Heath, A. Lozano, T. L. Marzetta, and P. Popovski, "Five disruptive technology directions for 5G," *IEEE Commun. Mag.*, vol. 52, no. 2, pp. 74–80, Feb. 2014.
- [5] Ofcom. *Spectrum Above 6 GHz for Future Mobile Communications*. Jan. 16, 2015. [Online]. Available: http://stakeholders.ofcom.org.uk/binaries/consultations/above-6ghz/summary/spectrum_above_6_GHz_CFI.pdf
- [6] W. Feng, Y. Li, D. Jin, L. Su, and S. Chen, "Millimetre-wave backhaul for 5G networks: Challenges and solutions," *Sensors*, vol. 16, no. 6, pp. 1–17, 2016.
- [7] P. Goel and K. J. Vinoy, "A low-cost phased array antenna integrated with phase shifters cofabricated on the laminate," *Progr. Electromagn. Res. B*, vol. 30, pp. 255–277, 2011.
- [8] M. Nikfalazar et al., "Steerable dielectric resonator phased-array antenna based on inkjet-printed tunable phase shifter with BST metal-insulator-metal varactors," *IEEE Antennas Wireless Propag. Lett.*, vol. 15, pp. 877–880, 2016.
- [9] Y. Yusuf and X. Gong, "A low-cost patch antenna phased array with analog beam steering using mutual coupling and reactive loading," *IEEE Antennas Wireless Propag. Lett.*, vol. 7, pp. 81–84, 2008.
- [10] H. Kawakami and T. Ohira, "Electrically steerable passive array radiator (ESPAR) antennas," *IEEE Antennas Propag. Mag.*, vol. 47, no. 2, pp. 43–50, Apr. 2005.
- [11] D.-T. Nguyen, R. Siragusa, and S. Tedjini, "Beam steering patch antenna using reactive loading and Yagi-antenna concept," *Microw. Opt. Technol. Lett.*, vol. 57, no. 2, pp. 417–421, 2015.

- [12] J. J. Luther, S. Ebadi, and X. Gong, "A microstrip patch electronically steerable parasitic array radiator (ESPAR) antenna with reactance-tuned coupling and maintained resonance," *IEEE Trans. Antennas Propag.*, vol. 60, no. 4, pp. 1803–1813, Apr. 2012.
- [13] M. R. Islam and M. Ali, "A 900 MHz beam steering parasitic antenna array for wearable wireless applications," *IEEE Trans. Antennas Propag.*, vol. 61, no. 9, pp. 4520–4527, Sep. 2013.
- [14] M. Jusoh, T. Aboufoul, T. Sabapathy, A. Alomainy, and M. R. Kamarudin, "Pattern-reconfigurable microstrip patch antenna with multidirectional beam for WiMAX application," *IEEE Antennas Wireless Propag. Lett.*, vol. 13, pp. 860–863, 2014.
- [15] M. R. Islam and M. Ali, "Elevation plane beam scanning of a novel parasitic array radiator antenna for 1900 MHz mobile handheld terminals," *IEEE Trans. Antennas Propag.*, vol. 58, no. 10, pp. 3344–3352, Oct. 2010.
- [16] N. M. Nor, M. H. Jamaluddin, M. R. Kamarudin, and M. Khalily, "Rectangular dielectric resonator antenna array for 28 GHz applications," *Progr. Electromagn. Res. C*, vol. 63, pp. 6–53, Apr. 2016.
- [17] M. R. Nikkiah, J. Rashed-Mohassel, and A. A. Kishk, "Compact low-cost phased array of dielectric resonator antenna using parasitic elements and capacitor loading," *IEEE Trans. Antennas Propag.*, vol. 61, no. 4, pp. 2318–2321, Apr. 2013.
- [18] N. H. Shahadan, M. R. Kamarudin, M. H. Jamaluddin, and Y. Y. Yamada, "Higher-order mode rectangular dielectric resonator antenna for 5G applications," *Indonesian J. Electr. Eng. Comput. Sci.*, vol. 5, no. 3, pp. 584–592, 2017.
- [19] N. H. Shahadan, M. R. Kamarudin, M. H. Jamaluddin, M. Khalily, and M. Jusoh, "Switched parasitic dielectric resonator antenna array using capacitor loading for 5G applications," in *Proc. 10th Eur. Conf. Antennas Propag. (EuCAP)*, 2016, pp. 1–5.
- [20] A. Petosa, *Dielectric Resonator Antenna Handbook*. Norwood, MA, USA: Artech House, 2007.
- [21] A. Petosa and S. Thirakoune, "Rectangular dielectric resonator antennas with enhanced gain," *IEEE Trans. Antennas Propag.*, vol. 59, no. 4, pp. 1385–1389, Apr. 2011.
- [22] R. Movahedinia, M. R. Chaharmir, A. R. Sebak, M. Ranjbar Nikkiah, and A. A. Kishk, "Realization of large dielectric resonator antenna ESPAR," *IEEE Trans. Antennas Propag.*, vol. 65, no. 7, pp. 3744–3749, Jul. 2017.
- [23] M. Ranjbar Nikkiah, P. Loghmannia, J. Rashed-Mohassel, and A. A. Kishk, "Theory of ESPAR design with their implementation in large arrays," *IEEE Trans. Antennas Propag.*, vol. 62, no. 6, pp. 3359–3364, Jun. 2014.



Ibrahim Sultan, Johor, Malaysia. Her research interests include dielectric resonator antenna design, steerable antenna, and switching.



He received the bachelor's and master's degrees in electrical engineering from Universiti Teknologi Malaysia, Malaysia, in 2003 and 2006, respectively, and the Ph.D. degree in signal processing and telecommunications from the Université de Rennes 1, France, in 2009, with a focus on microwave communication systems and specific antennas, such as a dielectric resonator and reflect array and dielectric dome antennas. He joined the Department of Electronic Engineering, Faculty of Electrical Engineering, Universiti Teknologi Malaysia, as a Tutor, in 2003. He is currently a Senior Lecturer with the Wireless Communication Centre, Faculty of Electrical Engineering, Universiti Teknologi Malaysia. He has authored over 40 ISI/Scopus papers in reputed indexed journals and also over 40 conference proceedings.



with the Wireless Communication Centre, Universiti Teknologi Malaysia, Malaysia, until 2017. He is currently a Senior Lecturer with the Centre for Electronic Warfare, Information and Cyber, Cranfield Defense and Security, Cranfield University, U.K. He holds a H-Index of 19 (SCOPUS) and over 1350 citations (SCOPUS). He has authored a book chapter of a book entitled *Antennas and Propagation for Body-Centric Wireless Communications* and has authored over 200 technical papers in journals and proceedings, including the IEEE TRANSACTION ON ANTENNAS AND PROPAGATION, the IEEE ANTENNAS AND WIRELESS PROPAGATION LETTERS, the IEEE Antenna Magazine, the IEEE ACCESS, the International Journal of Antennas and Propagation, the Progress in Electromagnetics Research, the Microwave and Optical Technology Letters, and Electronics Letters. His research interests include antenna design for 5G, wireless on-body communications, in-body communications (implantable antenna), RF and microwave communication systems, and antenna diversity. He is a Member of IET in 2011, an Executive Member of Antenna and Propagation (AP/MTT/EMC), Malaysia Chapter, and a Member of the IEEE Antennas and Propagation Society, the IEEE Communication Society, the IEEE Microwave Theory and Techniques Society, and the IEEE Electromagnetic Compatibility Society.



for terrestrial and satellite communications. From 1985 to 1993, he was involved on research and development of base station antennas for mobile radio systems. In 1993, he moved to NTT Mobile Communications Network Inc. (NTT DoCoMo). In 1995, he was temporarily transferred to YRP Mobile Telecommunications Key Technology Research Laboratories Co., Ltd. He was a Guest Professor with the Cooperative Research Center, Niigata University, and a Lecturer with the Tokyo University of Science, from 1996 to 1997. In 1998, he became a Professor with the National Defense Academy, Kanagawa, Japan. Since 2014, he has been a Professor with the Malaysia-Japan International Institute of Technology, Universiti Teknologi Malaysia, Kuala Lumpur, Malaysia. He is currently interested in very small antennas, array antennas, aperture antennas, and electromagnetic simulation of RCS. He received the Best Paper Award and the Best Tutorial Paper Award from the IEICE in 2013 and 2014, respectively. He is a Fellow Member of the IEICE and a Senior Member of the IEEE AP Society. He is also a member of the ACES.



His current research interests include dielectric resonator antennas, MIMO antennas, phased array antennas, and millimeter-wave antennas and propagation.

MUHAMMAD RAMLEE KAMARUDIN (M'08–SM'13) received the first degree (Hons.) in electrical and telecommunication engineering from Universiti Teknologi Malaysia (UTM), Johor Bahru, Malaysia, in 2003, the M.S. degree in communication engineering from the University of Birmingham, Birmingham, U.K., in 2004, and the Ph.D. degree from the University of Birmingham in 2007, under the supervision of Professor P. Hall. He was an Associate Professor

YOSHIHIDE YAMADA received the B.E. and M.E. degrees on electronics from the Nagoya Institute of Technology, Nagoya, Japan, in 1971 and 1973, respectively, and the D.E. degree in electrical engineering from the Tokyo Institute of Technology, Tokyo, Japan, in 1989. In 1973, he joined Electrical Communication Laboratories, Nippon Telegraph and Telephone Corporation (NTT). Until 1984, he was involved in research and development of reflector antennas

MOHSEN KHALILY (M'13) was with the Wireless Communication Center, Universiti Teknologi Malaysia, as a Senior Lecturer and a Post-Doctoral Research Fellow, from 2012 to 2015. He has been a Research Fellow with the Institute for Communication Systems, Home of 5G Innovation Center, University of Surrey, U.K., where he involved on antenna and propagation, since 2015. He has authored almost 60 academic papers in international peer-reviewed journals and conference proceedings.



MUZAMMIL JUSOH received the bachelor's degree in electrical-electronic and telecommunication engineering and the M.Sc. degree in electronic telecommunication engineering from Universiti Teknologi Malaysia in 2006 and 2010, respectively, and the Ph.D. degree in communication engineering from UniMAP in 2013. He was an RF and Microwave Engineer with Telekom Malaysia Berhad (TM) Company from 2006 to 2009. He is currently with Universiti Malaysia

Perlis (UniMAP) as a Senior Lecturer and a Researcher with the School of Computer and Communication Engineering. He is an Engineer (Team Leader) of Specialized Network Services Department based in TM Senai, Johor. He has been published in a number of quality journals, such as the IEEE AWPL, MOTL, IJAP, PIER, and Radio Engineering and over 70 conference papers. His research interests include antenna design, reconfigurable antenna, MIMO, UWB, and wireless communication system. He is currently supervising a number of Ph.D. and M.Sc. students and also managing few grants under Ministry of Higher Education Malaysia.



SAMSUL HAIMI DAHLAN received the Ph.D. degree in signal processing and telecommunications from the Universite de Rennes 1, France, in 2012. He has been a Senior Lecturer with the Faculty of Electric and Electronic Engineering, Universiti Tun Hussein Onn Malaysia (UTHM), since 2012. He is currently with the Research Center for Applied Electromagnetics, UTHM, as the Principal Researcher and has been the Head of the center since

2015. He has authored and co-authored papers for many journals, including the IEEE TRANSACTION ON ELECTROMAGNETIC COMPATIBILITY AND the IEEE AWPL. His research interests include Optical-Microwave generator, focusing system (dielectric lens and transmit array's synthesis), and computational electromagnetic technique, namely, the BOR-FDTD and material characterizations. He is supervising a number of bachelor's, master's, and Ph.D. students and is involved in several research projects sponsored by the industry and government agencies.

...